

Ultrafast thermionic emission from metal irradiated using a femtosecond laser and an electric field in combination

Tingfeng Wang, Jin Guo, Junfeng Shao, Dinan Wang, Anmin Chen, and Mingxing Jin

Citation: *Physics of Plasmas* **22**, 033106 (2015); doi: 10.1063/1.4914164

View online: <http://dx.doi.org/10.1063/1.4914164>

View Table of Contents: <http://scitation.aip.org/content/aip/journal/pop/22/3?ver=pdfcov>

Published by the *AIP Publishing*

Articles you may be interested in

[Ultrafast melting and resolidification of gold particle irradiated by pico- to femtosecond lasers](#)

J. Appl. Phys. **104**, 054910 (2008); 10.1063/1.2975972

[Periodic lines and holes produced in thin Au films by pulsed laser irradiation](#)

J. Appl. Phys. **100**, 044317 (2006); 10.1063/1.2234548

[Ultrafast dynamics of femtosecond laser-induced periodic surface pattern formation on metals](#)

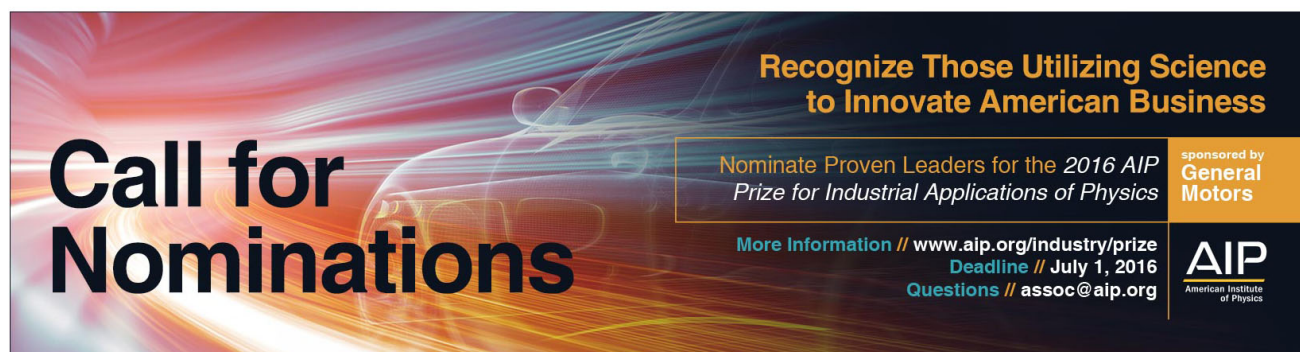
Appl. Phys. Lett. **87**, 251914 (2005); 10.1063/1.2146067

[Generation of wavelength-dependent, periodic line pattern in metal nanoparticle-containing polymer films by femtosecond laser irradiation](#)

Appl. Phys. Lett. **86**, 153111 (2005); 10.1063/1.1897052

[Surface thermal expansion of metal under femtosecond laser irradiation](#)

J. Appl. Phys. **82**, 5082 (1997); 10.1063/1.366382



Call for Nominations

Recognize Those Utilizing Science to Innovate American Business

Nominate Proven Leaders for the 2016 AIP Prize for Industrial Applications of Physics

More Information // www.aip.org/industry/prize
Deadline // July 1, 2016
Questions // assoc@aip.org

sponsored by General Motors

AIP
American Institute of Physics

Ultrafast thermionic emission from metal irradiated using a femtosecond laser and an electric field in combination

Tingfeng Wang,¹ Jin Guo,¹ Junfeng Shao,¹ Dinan Wang,¹ Anmin Chen,^{2,3,a)} and Mingxing Jin^{2,3,a)}

¹State Key Laboratory of Laser Interaction with Matter, Changchun Institute of Optics, Fine Mechanics and Physics, Chinese Academy of Sciences, Changchun 130033, China

²Institute of Atomic and Molecular Physics, Jilin University, Changchun 130012, China

³Jilin Provincial Key Laboratory of Applied Atomic and Molecular Spectroscopy (Jilin University), Changchun 130012, China

(Received 24 September 2014; accepted 23 February 2015; published online 6 March 2015)

Ultrafast thermionic emission from gold film irradiated with a femtosecond laser pulse in the presence of an additional electric field is analyzed using a two-temperature equation combined with a modified Richardson equation. The calculated results show that the duration of the emission is below 1 ps. Supplying an additional electric field is found to change the emission from the metal surface. Given the same laser fluence, this additional field reduces the work function of the metal, and thus improves the efficiency of thermionic emission. These results help to understand the mechanism and suggest ways to improve emissions in the context of ultrafast thermalized electron systems. © 2015 AIP Publishing LLC. [<http://dx.doi.org/10.1063/1.4914164>]

I. INTRODUCTION

Currently, the chirped-pulse amplification technique makes it possible to perform experiments with powerful femtosecond laser systems.¹ Many researchers have investigated the interaction between femtosecond laser pulses and metals for their potential applications.² In these studies, hot-electron relaxation dynamics is the focus of interest.^{3–5} For example, in the ultrashort burst of electrons created by the laser pulse, electrons are accelerated to kiloelectron volt energies by a dc electric field (ultrafast X-ray tube) or to gigaelectron volt energies by large-scale electron accelerator facilities (synchrotrons, free-electron lasers). These accelerated electrons generate X-rays via Bremsstrahlung radiation.⁶

A metal contains a large number of free electrons in the conduction band. If the temperature of the metal is increased, the electrons will move faster and some will have enough energy to escape from the metal surface.⁷ The energy to release a conduction-band electron from the metal surface is dependent on the properties of the metal.⁸ Higher temperature will generate escaping electrons with larger current, and this temperature induced electron emission is called thermionic emission. The physical dynamics is very complex during the femtosecond time interval that the laser irradiates the metal.⁹ The temperature of electrons on the surface of the metal after irradiation increases rapidly within an extremely short time. Because the specific heat capacity of electrons is much lower than that of the lattice, a greater temperature difference between electrons and lattice is produced. This process establishes a nonequilibrium state within the femtosecond laser heated metal, the dynamics of which are driven by the electron-lattice coupling.¹⁰ Based

on this mechanism, many applications can be realized exploiting laser-induced electron emissions, including ultra-short X-ray pulse generation^{11,12} and laser-driven electron sources.^{13,14} The mechanism of thermionic emission in femtosecond laser irradiation metal has been widely studied by many researchers.^{15–17} It is a great challenge to increase thermionic emissions in the various applications. From its physical nature,^{18,19} at higher temperatures, the emitted electrons mainly come from the metal surface as these electrons can overcome the potential barrier, that is, the work function of the metal. If the potential energy barrier was lowered, more electrons would escape and thereby the thermionic emissions would improve.

In our study, an additional electric field is introduced during thermionic emissions to verify this idea. Moreover, femtosecond laser heating of a gold film is investigated numerically. The calculated results indicate that the additional electric field can enhance thermionic emissions from the surface of the metal, and hence its emission efficiency.

II. MATHEMATICAL MODEL

A. Two-temperature model

For femtosecond laser heating of metals, because the full width at half maximum (FWHM) of femtosecond laser pulses is significantly shorter than the relaxation time between electron and lattice, the conventional heat conduction equation fails to solve this problem. To resolve the issue, Anisimov *et al.* proposed the two-temperature model,²⁰ which describes the interaction between the ultrashort laser pulses and the metal. The physical process can be divided into two stages: First, the laser energy is absorbed by free electrons; second, energy is transferred from the free electrons to the lattice.^{20–22} The one-dimensional two-temperature equations are given as^{23–25}

^{a)}Authors to whom correspondence should be addressed. Electronic addresses: amchen@jlu.edu.cn and mxjin@jlu.edu.cn.

$$C_e \frac{\partial T_e}{\partial t} = \frac{\partial}{\partial x} \left(k_e \frac{\partial T_e}{\partial x} \right) - G(T_e - T_l) + S, \quad (1)$$

$$C_l \frac{\partial T_l}{\partial t} = \frac{\partial}{\partial x} \left(k_l \frac{\partial T_l}{\partial x} \right) + G(T_e - T_l), \quad (2)$$

where T_e is the temperature of electron, T_l the temperature of lattice, t the time variable, x the depth from the metal surface, and $C_e = \gamma T_e$ the electron heat capacity.²⁶ In metals, the mechanism of heat conduction is mainly determined by electrons.²⁷ C_l , the heat capacity of lattice, can be considered as constant.²⁸ Also, $k_e = k_{e0} B T_e / (A T_e^2 + B T_l)$ is electron thermal conductivity,²⁸ where k_{e0} , A , and B are the material constants. $G = G_0 (A(T_e + T_l) / B + 1)$ is the electron-lattice coupling factor,²⁹ where G_0 is the coupling factor at room temperature.^{30,31} S is the laser heat source, which can be modeled with a Gaussian temporal profile³²

$$S = \sqrt{\frac{\beta(1-R)I}{\pi t_p \alpha}} \exp \left[-\frac{x}{\alpha} - \beta \left(\frac{t - 2t_p}{t_p} \right)^2 \right], \quad (3)$$

where t_p is the FWHM, R the target reflection coefficient, α the penetration depth, I the incident energy, and $\beta = 4 \ln(2)$.

B. Thermionic emission

If the temperature of the conduction electrons in the metal is high enough, the tail part of the Fermi-Dirac distribution crosses the vacuum level, and hence thermionic electron emission begins. The rate of thermionic emission from metal is represented by the Richardson equation^{17,33,34}

$$J = \left(\frac{4\pi m}{h^3} \right) (k_B T_e)^2 \exp \left[-\frac{W}{k_B T_e} \right], \quad (4)$$

where k_B is the Boltzmann constant, $W = e\phi$ with e is the charge of an electron and ϕ is the work function of the metal.³⁵ m the mass of the electron, and h the Planck constant.

When a large number of electrons are produced over the metal surface, space-charge effects occur because of the Coulomb interactions from the emitted electrons.³⁶ Riffe *et al.* included an effective space-charge potential with the inner potential to take electron removal from the metal into consideration. For this reason, Eq. (4) is modified to give the Richardson–Dushman equation^{16,37}

$$J = \left(\frac{4\pi m}{h^3} \right) (k_B T_e)^2 \exp \left[-\frac{W + W_{sc}}{k_B T_e} \right], \quad (5)$$

where $W_{sc} = a N e^2 / R_1$ is the space-charge potential, $a = 1.95$ a geometry specific constant,³⁷ and N the total number of electrons emitted from the surface region. This is given by the following expression:^{16,37}

$$N = \frac{k_B T_e}{a e^2 / R_1} \log \left[1 + \frac{4\pi m}{h^3} t_p \pi R_2 a e^2 k_B T_e \exp \left(-\frac{W}{k_B T_e} \right) \right], \quad (6)$$

where R_1 and R_2 are the lengths of the semi-major and semi-minor axes of the electron-charge disk.³⁷

TABLE I. Thermal and optical physical parameters for gold.

Electron-lattice coupling coefficient $G_0 (10^{17} \text{Jm}^{-3} \text{s}^{-1} \text{K}^{-1})$	0.22
Electron heat capacity coefficient $\gamma (\text{Jm}^{-3} \text{K}^{-2})$	68
Electron thermal conductivity coefficient $k_{e0} (\text{Jm}^{-1} \text{s}^{-1} \text{K}^{-1})$	315
Lattice heat capacity $C_l (10^6 \text{Jm}^{-3} \text{K}^{-1})$	2.5
Penetration depth $\alpha (10^{-9} \text{m})$	15.3
$A (10^7 \text{s}^{-1} \text{K}^{-2})$	1.18
$B (10^{11} \text{s}^{-1} \text{K}^{-1})$	1.25
Work function $\phi (\text{eV})$	5.4

In electron emissions, an electric field of magnitude F at the metal surface is added normal to the surface. Without the field, the surface barrier generated by an escaping Fermi-level electron has energy W , which is equal to the local work function. The electric field lowers the surface barrier energy by an amount ΔW , and thus increases the emission current,³⁸ this is known as the Schottky effect³⁹ (named after Walter H. Schottky) or field-enhanced thermionic emission. The Schottky effect reduces the barrier and increases the electron yield, and can be modeled by a simple modification of the Richardson equation by replacing W by $W - \Delta W$.^{40,41} With the above factors being considered, we obtain the following equation:^{38,42}

$$J = \left(\frac{4\pi m}{h^3} \right) (k_B T_e)^2 \exp \left[-\frac{W + W_{sc} - \Delta W}{k_B T_e} \right], \quad (7)$$

where $\Delta W = e \sqrt{eF / 4\pi \epsilon_0}$ ^{41,42} and ϵ_0 is the vacuum permittivity.

III. RESULT AND DISCUSSION

In our study, a gold film with surface reflectivity $R = 0.974$ and thickness of 100 nm was used as the metal sample and the laser light source used to irradiate the sample was a 100 fs laser with wavelength of 800 nm with laser fluence of 100 mJ/cm². Before irradiation, the initial temperature of the electron and lattice was considered the same at $T_0 = 300 \text{K}$. The values of the thermal physical parameters used in the calculation are listed in Table I.^{8,43} The time-dependence of the calculated electron and lattice temperature on the surface of gold film (Fig. 1) shows that the electron temperature rises rapidly up to a maximum value at the

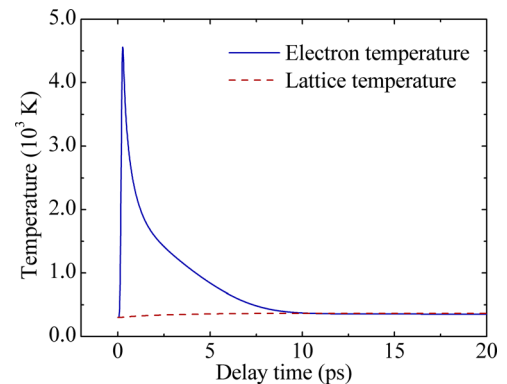


FIG. 1. Evolution of electron and lattice temperature with the delay time at the metal surface. The laser fluence is 100 mJ/cm².

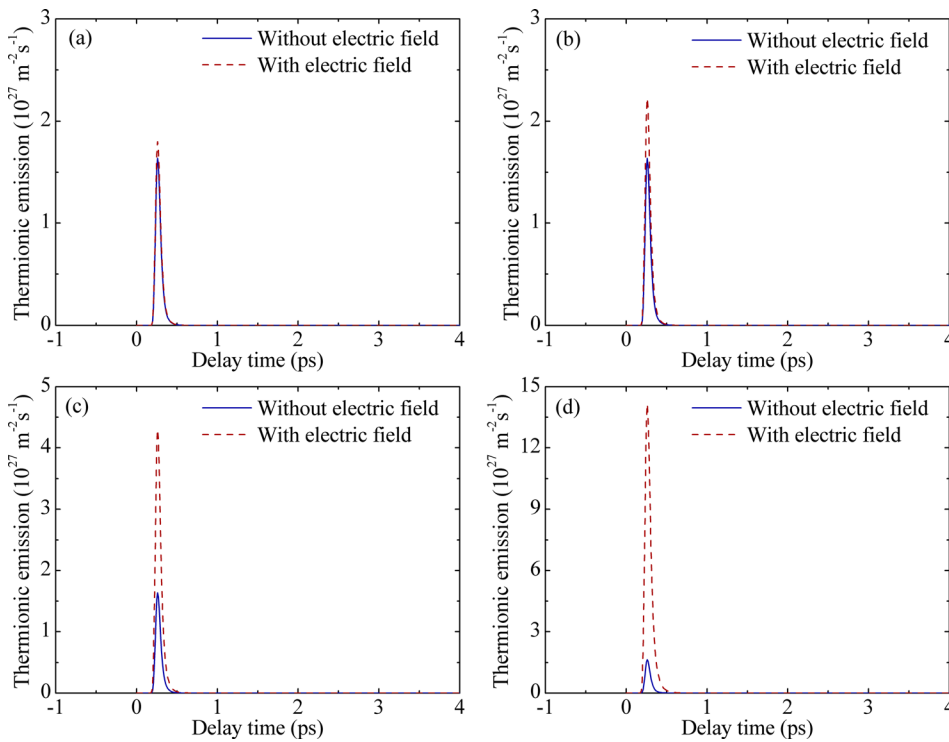


FIG. 2. Evolution of the thermionic emission with the delay time at the same laser fluence (100 mJ/cm^2). The strengths of the electric field are 0.001 V/nm (a), 0.01 V/nm (b), 0.1 V/nm (c), and 0.5 V/nm (d).

surface. After pulse irradiation, the surface electron temperature decreases with time as heat diffuses with the freeing of the electron gas.^{25,28} Finally, the system reaches its thermal equilibrium at the delay time of about 10 ps.

Figure 2 shows the calculated temporal evolution of the thermionic emission as obtained from Fig. 1 and calculated using Eqs. (4) and (5) with different electric fields. The laser fluence is set to 100 mJ/cm^2 , and the strengths of electric fields are 0.001 V/nm, 0.01 V/nm, 0.1 V/nm, and 0.5 V/nm. From Fig. 2, the duration of the thermionic emission is

clearly subpicosecond. Such thermionic emissions have been used for the generation of ultrashort electron beam pulses and X-rays.⁴⁴ A direct comparison between the thermionic emission pulse shape calculated without electric field (solid line) and that calculated with different electric field (dashed line) is also presented in this figure. It indicates that the peak intensity of thermionic emission is significantly improved by increasing the intensity of electric field. The electric-field-enhanced thermionic emission combines the electric field effect and thermionic effect into a single physical process to

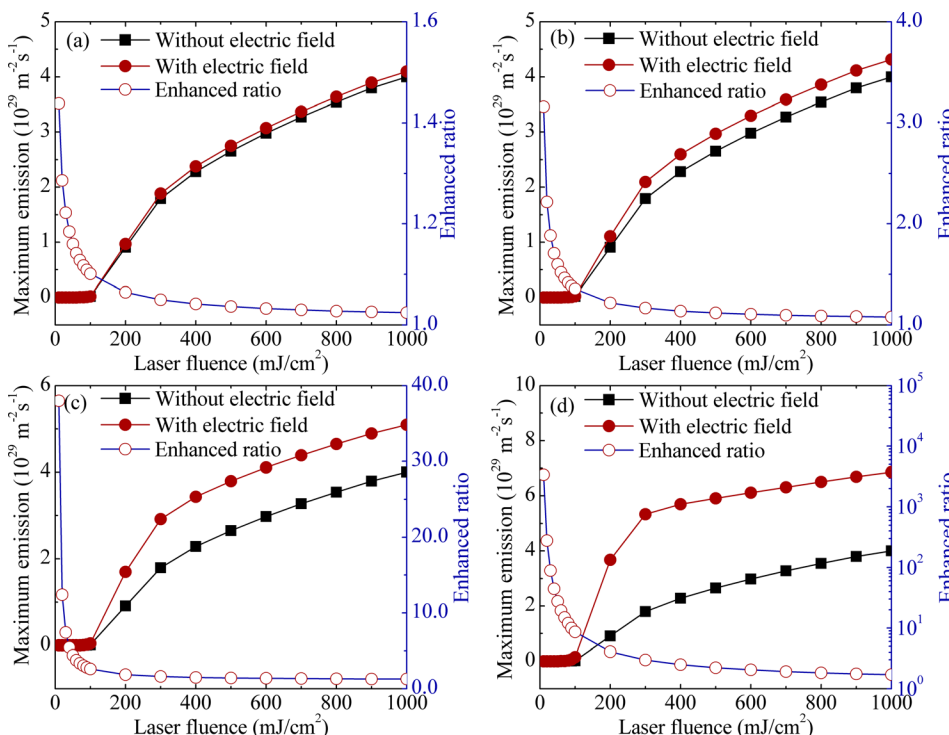


FIG. 3. Maximum thermionic emission (left axes) and the enhancement ratio (right axes) as a function of laser fluence with and without the electric field. The strength of the electric field is 0.001 V/nm (a), 0.01 V/nm (b), 0.1 V/nm (c), and 0.5 V/nm (d).

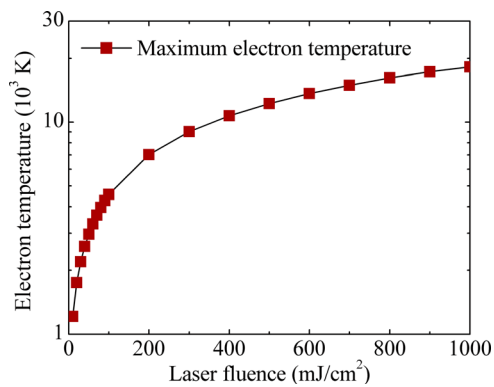


FIG. 4. Maximum electron temperature as a function of laser fluence at the surface.

make use of both a high electric field and available thermal energy coming from the laser-heated electrons.^{37,45} Ultrafast thermionic emission occurred during a simple two-step process. The first step is the absorption of laser energy by the electrons within the femtosecond pulse duration. Note that it takes a few femtoseconds for the electrons to reestablish the Fermi distribution, the electrons obtain very high temperatures, whereas the lattice of the metal remains undisturbed. In the second step, the higher temperature electrons overcome the binding potential, and electron emission then takes place. Note here that the energy begins to be transferred from the electron to the lattice through the electron-lattice coupling, and the electron temperature starts to decrease rapidly. As a result, the electrons will not have enough energy to overcome the barrier, and thus a cut-off in the electron emission is established. The duration of the electron emission generated from the irradiated metal is subpicosecond.⁴⁶ Although the electron-lattice relaxation time is around tens of picoseconds,^{9,22} in the process of electric field enhanced thermionic emission, more electrons with energies greater

than the electron affinity arrive at the surface and are emitted into the vacuum and collected, thereby generating higher current (Fig. 2). Thus, each emitted electron has absorbed sufficient laser energy and is thermalized to overcome the electron affinity of metal in the electric field. Introducing an additional electric field is equivalent to reducing the binding potential of the metal.

Figure 3 shows the evolution of maximum thermionic emission and emission enhancement ratio with the laser fluence for different electric fields, where the field intensities are 0.001 V/nm (a), 0.01 V/nm (b), 0.1 V/nm (c), and 0.5 V/nm (d). Here, the enhancement ratio is defined as the ratio of the thermionic emission with the electric field to that without the electric field. Figure 4 shows the maximum electron temperature with the laser fluence on the surface. From Figs. 3 and 4, both maximum electron temperature and maximum thermionic emission increase with increasing laser fluence. In these cases, it should be noted that thermionic emission increases at a faster rate with increasing intensity of the electric field. For femtosecond laser-heated metal, the electrons on the metal surface can obtain higher temperatures by increasing laser fluence.⁴⁷ Because the temperature of the electron at the surface determines the thermionic electron emission,⁴⁸ the increase in laser fluence will result in a marked increase in thermionic emission. However, the enhancement ratio quickly decreases as laser fluence is increased. If the laser fluence is about 100 mJ/cm², the decay of the enhancement ratio becomes slower, while thermionic emissions increase more rapidly. The enhancement effect from the added electric field is weakened at higher laser fluence. This is because a large number of electrons have obtained enough energy to overcome the binding potential of metal under the higher laser irradiation. From Fig. 3(d), the maximum emission almost remains constant for an electric field of 0.5 V/nm and with increasing laser fluence to about

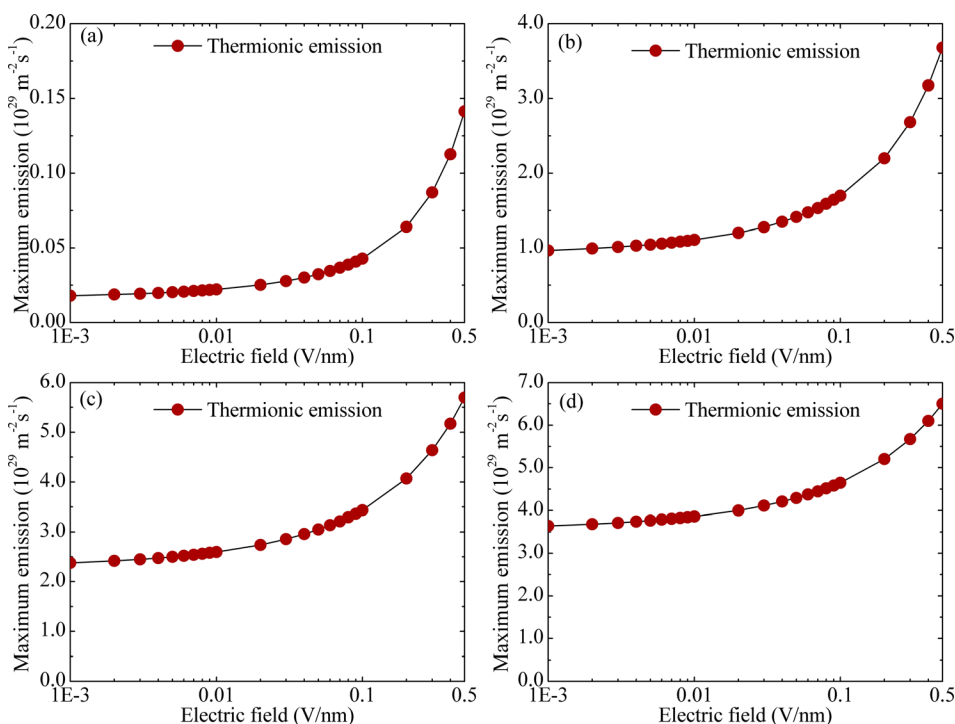


FIG. 5. Maximum thermionic emission as a function of the electric field. The laser fluences are 100 mJ/cm² (a), 200 mJ/cm² (b), 400 mJ/cm² (c), and 800 mJ/cm² (d).

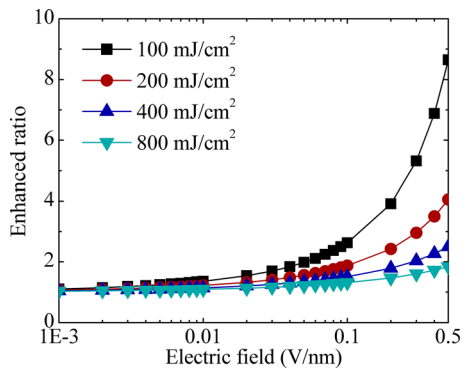


FIG. 6. Enhancement ratio as a function of the electric field at different laser fluences of 100 mJ/cm², 200 mJ/cm², 400 mJ/cm², and 800 mJ/cm².

300 mJ/cm². This is because no more electrons can escape from the metal surface because of space-charge effects.

Figure 5 shows the maximum thermionic emission with the electric field at different laser fluences, specifically 100 mJ/cm² (a), 200 mJ/cm² (b), 400 mJ/cm² (c), and 800 mJ/cm² (d). Increasing the electric field clearly increases the thermionic emission. Although the total laser energy delivered to gold film is the same for each case, the increase in electric field strength results in a rapid increase in thermionic emission. For the electron emission, it is essential to use the electric field to reduce the binding potential of metal for the electrons. The enhancement ratio calculated from Fig. 5 is plotted in Fig. 6. At the laser fluence of 100 mJ/cm², the enhancement ratio has increased to about 20. However, the maximum enhancement ratio is only about 2 at the laser fluence of 800 mJ/cm². The results reveal that the thermionic electron emission enhanced by the external electric field is very significant at lower femtosecond laser fluence, and the increase in laser fluence slightly improves thermionic electron emission.

IV. CONCLUSION

In conclusion, a numerical solution of the two-temperature model combined with a modified Richardson equation has been performed to investigate the thermionic emission from gold film heated using a femtosecond laser. A direct comparison between the thermionic emission pulse shape calculated without electric field and that calculated with additional electric field at the same laser energy was presented. The duration of the thermionic emission is subpicosecond. Compared with the thermionic emission produced without additional electric field, the electric field produces an enhanced thermionic emission from the metal under femtosecond laser irradiation. Indeed, introducing this additional field is equivalent to reducing the binding potential of metal. The enhanced efficiency of thermionic emission can be further increased by increasing the intensity of the electric field; however, the enhancement ratio decreases with increasing laser fluence. The calculated results reveal that the electric-field-enhanced ultrafast thermionic emissions generated by lower femtosecond laser fluences are substantial enough to warrant use in applications. Such enhanced emissions can

efficiently improve the generated efficiency of ultrashort electron beam pulses and X-rays.

ACKNOWLEDGMENTS

This project was supported by the National Basic Research Program of China (973 Program, Grant No. 2013CB922200), the China Postdoctoral Science Foundation (Grant No. 2014M551169), the Fundamental Research Funds for the Central Universities, and the National Natural Science Foundation of China (Grant Nos. 10974069 and 11034003).

- ¹D. Strickland and G. Mourou, *Opt. Commun.* **56**, 219 (1985).
- ²A. V. Lugovskoy and I. Bray, *Phys. Rev. B* **60**, 3279 (1999).
- ³C. Kealhofer, S. M. Foreman, S. Gerlich, and M. A. Kasevich, *Phys. Rev. B* **86**, 035405 (2012).
- ⁴Z. Y. Chen, J. F. Li, Y. Yu, J. X. Wang, X. Y. Li, Q. X. Peng, and W. J. Zhu, *Phys. Plasmas* **19**, 113116 (2012).
- ⁵L. M. Chen, J. Zhang, Q. L. Dong, H. Teng, T. J. Liang, L. Z. Zhao, and Z. Y. Wei, *Phys. Plasmas* **8**, 2925 (2001).
- ⁶A. Egbert, B. N. Chichkov, and A. Ostendorf, *Europhys. Lett.* **56**, 228 (2001).
- ⁷E. L. Murphy and R. H. Good, *Phys. Rev.* **102**, 1464 (1956).
- ⁸D. R. Lide, *CRC Handbook of Chemistry and Physics*, 84th ed. (CRC Press, Boca Raton, 2003).
- ⁹B. Rethfeld, K. Sokolowski-Tinten, D. von der Linde, and S. I. Anisimov, *Appl. Phys. A* **79**, 767 (2004).
- ¹⁰B. H. Christensen, K. Vestentoft, and P. Balling, *Appl. Surf. Sci.* **253**, 6347 (2007).
- ¹¹Z. S. Tao, H. Zhang, P. M. Duxbury, M. Berz, and C. Y. Ruan, *J. Appl. Phys.* **111**, 044316 (2012).
- ¹²J. F. Seely, C. I. Szabo, P. Audebert, E. Brambrink, E. Tabakhoff, and L. T. Hudson, *Phys. Plasmas* **17**, 023102 (2010).
- ¹³V. Ayvazyan, N. Baboi, I. Bohnet, R. Brinkmann, M. Castellano, P. Castro, L. Catani, S. Choroba, A. Cianchi, M. Dohlus, H. T. Edwards, B. Faatz, A. A. Fateev, J. Feldhaus, K. Flottmann, A. Gamp, T. Garvey, H. Genz, C. Gerth, V. Gretchko, B. Grigoryan, U. Hahn, C. Hessler, K. Honkavaara, M. Huning, R. Ischebeck, M. Jablonka, T. Kamps, M. Korfer, M. Krassilnikov, J. Krzywinski, M. Liepe, A. Liero, T. Limberg, H. Loos, M. Luong, C. Magne, J. Menzel, P. Michelato, M. Minty, U. C. Muller, D. Nolle, A. Novokhatski, C. Pagani, F. Peters, J. Pfluger, P. Piot, L. Plucinski, K. Rehlich, I. Reyzl, A. Richter, J. Rossbach, E. L. Saldin, W. Sandner, H. Schlarb, G. Schmidt, P. Schmuser, J. R. Schneider, E. A. Schneidmiller, H. J. Schreiber, S. Schreiber, D. Sertore, S. Setzer, S. Simrock, R. Sobierajski, B. Sonntag, B. Steeg, F. Stephan, K. P. Sytchev, K. Tiedtke, M. Tonutti, R. Treusch, D. Trines, D. Turke, V. Verzilov, R. Wanzenberg, T. Weiland, H. Weise, M. Wendt, I. Will, S. Wolff, K. Wittenburg, M. V. Yurkov, and K. Zapfe, *Phys. Rev. Lett.* **88**, 104802 (2002).
- ¹⁴X. J. Wang, D. Xiang, T. K. Kim, and H. Ihee, *J. Korean Phys. Soc.* **48**, 390 (2006).
- ¹⁵X. Y. Wang, D. M. Riffe, Y. S. Lee, and M. C. Downer, *Phys. Rev. B* **50**, 8016 (1994).
- ¹⁶D. M. Riffe, X. Y. Wang, M. C. Downer, D. L. Fisher, K. Tajima, and J. L. Erskine, *J. Opt. Soc. Am. B* **10**, 1424 (1993).
- ¹⁷G. Q. Du, Q. Yang, F. Chen, X. W. Meng, H. Bian, J. H. Si, and X. Hou, *Appl. Phys. A* **112**, 479 (2013).
- ¹⁸E. B. Yakovlev, O. N. Sergaeva, and V. V. Svirina, *J. Opt. Technol.* **78**, 487 (2011).
- ¹⁹S. G. Bezhakov, A. P. Kanavin, and S. A. Uryupin, *Quant. Electron.* **42**, 447 (2012).
- ²⁰S. I. Anisimov, B. L. Kapeliovich, and T. L. Perelman, *Sov. J. Exp. Theor. Phys.* **39**, 375 (1974), see <http://www.jetp.ac.ru/cgi-bin/e/index/e/39/2/p375?a=list>.
- ²¹S. Y. Wang, Y. Ren, C. W. Cheng, J. K. Chen, and D. Y. Tzou, *Appl. Surf. Sci.* **265**, 302 (2013).
- ²²Y. Gan and J. K. Chen, *Opt. Lett.* **37**, 2691 (2012).
- ²³Y. Gan and J. K. Chen, *Appl. Phys. Lett.* **94**, 201116 (2009).
- ²⁴P. B. Corkum, F. Brunel, N. K. Sherman, and T. Srinivasan-Rao, *Phys. Rev. Lett.* **61**, 2886 (1988).

- ²⁵J. K. Chen and J. E. Beraun, *J. Opt. A* **5**, 168 (2003).
- ²⁶J. Kim and S. Na, *Opt. Laser Technol.* **39**, 1443 (2007).
- ²⁷Y. W. Zhang and J. K. Chen, *J. Appl. Phys.* **104**, 054910 (2008).
- ²⁸Y. Yamashita, T. Yokomine, S. Ebara, and A. Shimizu, *Fusion Eng. Des.* **81**, 1695 (2006).
- ²⁹P. B. Allen, *Phys. Rev. Lett.* **59**, 1460 (1987).
- ³⁰P. E. Hopkins and P. M. Norris, *Appl. Surf. Sci.* **253**, 6289 (2007).
- ³¹J. Huang, Y. W. Zhang, and J. K. Chen, *Appl. Phys. A* **95**, 643 (2009).
- ³²A. A. Unal, A. Stalmashonak, G. Seifert, and H. Graener, *Phys. Rev. B* **79**, 115411 (2009).
- ³³S. S. Mao, X. Mao, R. Greif, and R. E. Russo, *Appl. Phys. Lett.* **73**, 1331 (1998).
- ³⁴J. Guo, T. F. Wang, J. F. Shao, T. Sun, R. Wang, A. M. Chen, Z. Hu, M. X. Jin, and D. J. Ding, *Opt. Commun.* **285**, 1895 (2012).
- ³⁵W. M. H. Sachtler, G. J. H. Dorgelo, and A. A. Holscher, *Surf. Sci.* **5**, 221 (1966).
- ³⁶W. Wendelen, B. Y. Mueller, D. Autrique, A. Bogaerts, and B. Rethfeld, *Appl. Phys. Lett.* **103**, 221603 (2013).
- ³⁷T. Balasubramni, S. H. Kim, and S. H. Jeong, *Appl. Surf. Sci.* **255**, 9601 (2009).
- ³⁸N. Spyropoulos-Antonakakis, E. Sarantopoulou, Z. Kollia, Z. Samardzija, S. Kobe, and A. C. Cefalas, *J. Appl. Phys.* **112**, 094301 (2012).
- ³⁹J. Orloff, *Handbook of Charged Particle Optics* (CRC press, 2008).
- ⁴⁰M. E. Kiziroglou, X. Li, A. A. Zhukov, R. A. J. de Groot, and C. H. de Groot, *Solid-State Electron.* **52**, 1032 (2008).
- ⁴¹D. H. Dowell and J. F. Schmerge, *Phys. Rev. ST Accel Beams* **12**, 074201 (2009).
- ⁴²G. Caretto, D. Doria, V. Nassisi, and M. V. Siciliano, *J. Appl. Phys.* **101**, 073109 (2007).
- ⁴³J. Huang, Y. W. Zhang, and J. K. Chen, *Trans. ASME J. Heat Transfer* **134**, 012401 (2012).
- ⁴⁴T. Pfeifer, C. Spielmann, and G. Gerber, *Rep. Progr. Phys.* **69**, 443 (2006).
- ⁴⁵G. Q. Du, Q. Yang, F. Chen, J. H. Si, and X. Hou, *Appl. Surf. Sci.* **257**, 9177 (2011).
- ⁴⁶U. Hinze, A. Egbert, B. Chichkov, and K. Eidmann, *Opt. Lett.* **29**, 2079 (2004).
- ⁴⁷A. Egbert, B. Mader, B. Tkachenko, C. Fallnich, B. N. Chichkov, H. Stiel, and P. V. Nickles, *Appl. Phys. Lett.* **81**, 2328 (2002).
- ⁴⁸J. Domenech-Garret, S. Tierno, and L. Conde, *Eur. Phys. J. B* **86**, 382 (2013).